

Band Hybridization Induced Odd-Frequency Pairing in Multiband Superconductors

L. Komendová,¹ A. V. Balatsky,^{2,3} and A. M. Black-Schaffer¹

¹*Department of Physics and Astronomy, Uppsala University, Box 530, SE-751 21 Uppsala*

²*NORDITA, Center for Quantum Materials, KTH Royal Institute of Technology,
and Stockholm University, Roslagstullsbacken 23, SE-106 91 Stockholm, Sweden*

³*Institute for Materials Science, Los Alamos National Laboratory, Los Alamos, NM 87545, United States*

(Dated: September 18, 2018)

We investigate how hybridization (single-quasiparticle scattering) between two superconducting bands induces odd-frequency superconductivity in a multiband superconductor. An explicit derivation of the odd-frequency pairing correlation and its full frequency dependence is given. We find that the density of states is modified, from the sum of the two BCS spectra, at higher energies by additional hybridization gaps with strong coherence peaks when odd-frequency pairing is present.

Many materials have multiple bands close to the Fermi level. It is then not surprising that there also exist many superconductors with more than one superconducting band. Well-known multiband superconductors are MgB₂ [1–3], which hosts two distinct superconducting gaps, and the iron-based superconductors [4–6], where the order parameter changes sign between different bands [7, 8]. Multiband superconductivity has also been suggested to be important in simple metals [9, 10], heavy fermion compounds [11–15], different carbides [16, 17], and Chevrel phases [18], as well as for engineering time-reversal invariant topological superconducting states [19, 20].

Multiple superconducting bands allow for unusual coupling effects. Early, and much current, theoretical focus has been oriented towards studying the effects of Josephson coupling between different superconducting bands, i.e. the exchange of whole Cooper pairs between bands [21–26]. However, conceptually much simpler is single-quasiparticle scattering, or tunneling, between the superconducting bands. The origin of interband quasiparticle scattering can be impurity scattering, but a common intrinsic source is superconductivity associated with specific orbitals, which subsequently hybridize to form the low-energy bands around the Fermi surface. Tunneling spectroscopy has found significant effects of interband quasiparticle scattering in silicon clathrate Ba₈Si₄₆ [27, 28], iron-based superconductors [29], and MgB₂ [30]. Recent ARPES data on MgB₂ have also shown that interband scattering due to disorder can be important [31].

Theoretically, interband single-quasiparticle scattering results in both band hybridization and *interband* pairing, where the two electrons forming a Cooper pair belong to *different* bands. Straightforward effects of band hybridization were studied already quite early on [32–34]. More recently, band hybridization has also been proposed to influence the nodal structure of the superconducting gap in iron-based superconductors [35–38]. On the other hand, consequences of the induced interband pairing have been much less discussed. Pure interband pairing in cold atoms and quantum chromodynamics systems has been proposed to give a “breached” regime containing both a superfluid and a normal liquid [39, 40], however, in band-

hybridized superconductors the interband pairing is also accompanied by (usually large) conventional intraband pairings. Still, it was recently pointed out, using symmetry arguments and simple mean-field BCS calculations, that odd-frequency, odd-interband pairing can be ubiquitous in multiband superconductors [41].

The fermionic nature of the superconducting wave function usually renders a division into spin-singlet even-parity (i.e. *s*-, *d*-wave) or spin-triplet odd-parity (*p*-wave) superconductors, but it can also be even or odd under time, or equivalently frequency [42–44]. Examples of this are odd-frequency spin-triplet *s*-wave superconductivity giving rise to long-scale proximity effects in superconductor-ferromagnet systems [45–47] or odd-frequency spin-singlet *p*-wave pairing in non-magnetic junctions [48–50]. In multiband superconductors the band index offers the additional possibility of spin-singlet *s*-wave pairing which is odd in both band and frequency, without translation or spin rotation symmetry breaking.

In this work we derive the exact Green’s functions for a generic multiband superconductor with single-quasiparticle scattering. We thus obtain the full frequency dependence of the interband pairing and find that the odd-interband pairing has odd frequency dependence, while the even-interband pairing is even in frequency. By studying the density of states (DOS) we also discover that finite band hybridization gives rise to an extra gap located beyond the original gap edges. This hybridization-induced gap is not fully depleted, but has very pronounced BCS-like coherence peaks. Moreover, the hybridization gap disappears whenever the odd-frequency interband pairing is zero and is thus a directly measurable signal of odd-frequency superconductivity.

To model a generic multiband superconductor we consider two bands, band 1 and 2, with dispersions ϵ_{k1} and ϵ_{k2} , where $\epsilon_k = \epsilon_{-k}$. For simplicity, we assume that the two bands independently develop conventional spin-singlet *s*-wave superconducting order parameters Δ_1 and Δ_2 , respectively, but one of them can also be zero. Finally, we add a small single-quasiparticle hybridization, or scattering, term proportional to Γ between the two

bands, resulting in the Hamiltonian:

$$H = \sum_{k\sigma} \epsilon_{k1} a_{k\sigma}^\dagger a_{k\sigma} + \epsilon_{k2} b_{k\sigma}^\dagger b_{k\sigma} + \sum_{k\sigma} \Gamma(k) a_{k\sigma}^\dagger b_{k\sigma} + \text{H.c.} \\ + \sum_k \Delta_1(k) a_{k\uparrow}^\dagger a_{-k\downarrow}^\dagger + \Delta_2(k) b_{k\uparrow}^\dagger b_{-k\downarrow}^\dagger + \text{H.c.}, \quad (1)$$

where a (b) is the annihilation operator in band 1 (2). Alternatively, the band hybridization can be interpreted as a coupling process in real space, with the a - and b -electrons living to the left and the right of a junction or in different layers [32, 51]. In this picture the Josephson coupling would instead be a two-particle tunneling term (not included here).

We start by calculating the spin-singlet s -wave interband anomalous Green's functions F_{12} and F_{21} , which express the pairing correlations of two electrons belonging to different bands. Assuming Γ to be a small parameter, we can use standard perturbation theory [52]. The first order contributions are then represented by the schematic diagrams in the inset of Fig. 1(a) and give: $F_{12}^{(1)} = F_1 \Gamma G_2 - \overleftarrow{G}_1 \Gamma F_2$, where \overleftarrow{G} is the hole propagator, i.e., $\overleftarrow{G} = -G(-k, -\omega)$. The minus sign before the second term is due to scattering of hole propagators (left-going arrows). The normal and anomalous propagators without the hybridization are as usual [52]:

$$\begin{pmatrix} G_j & F_j \\ F_j^\dagger & \overleftarrow{G}_j \end{pmatrix} = \frac{1}{(i\omega)^2 - E_j^2} \begin{pmatrix} i\omega + \epsilon_{kj} & \Delta_j \\ \Delta_j^* & i\omega - \epsilon_{kj} \end{pmatrix}, \quad (2)$$

where $E_j^2 = E_{kj}^2 = \epsilon_{kj}^2 + |\Delta_j|^2$ and $\omega = \omega_n = \pi(2n + 1)k_B T$ are the fermionic Matsubara frequencies. Using these expressions we arrive at $F_{12}^{(1)} = \Gamma[i\omega(\Delta_1 - \Delta_2) + \Delta_1\epsilon_{k2} + \Delta_2\epsilon_{k1}]/[(\omega^2 + E_1^2)(\omega^2 + E_2^2)]$. The next to leading order terms for F_{12} are cubic in Γ . Further organizing the perturbation expansion of the interband pairing of a given order n in a systematic way, we find several recursion relationships [61]. These can be compactly written in a matrix form as:

$$\begin{pmatrix} \overleftarrow{G}_{12}^{(n)} \\ F_{12}^{(n)} \end{pmatrix} = g \begin{pmatrix} e & f \\ -f^* & e^* \end{pmatrix} \begin{pmatrix} \overleftarrow{G}_{12}^{(n-2)} \\ F_{12}^{(n-2)} \end{pmatrix}, \quad (3)$$

where $g = \Gamma^2/[(\omega^2 + E_{k1}^2)(\omega^2 + E_{k2}^2)]$, $e = (i\omega - \epsilon_1)(i\omega - \epsilon_2) - \Delta_1\Delta_2^*$ and $f = -i\omega(\Delta_1^* - \Delta_2^*) + \Delta_1^*\epsilon_2 + \Delta_2^*\epsilon_1$. For the starting point of the recursion we use the first order anomalous interband Green's function $F_{12}^{(1)}$ and the corresponding normal propagator: $\overleftarrow{G}_{12}^{(1)} = \Gamma[\Delta_1\Delta_2^* - (i\omega - \epsilon_1)(i\omega - \epsilon_2)]/[(\omega^2 + E_1^2)(\omega^2 + E_2^2)]$. From Eq. (3) we recognize that the Green's functions to infinite order can be written as a geometric series, where the quotient is a two-by-two matrix. The formal criterion for a matrix geometric series to be convergent is that the norm (i.e. the largest singular value) of the coefficient matrix is < 1 . From this we arrive at the condition

$\Gamma \lesssim (\omega^2 + E_1^2)^{1/4}(\omega^2 + E_2^2)^{1/4}$, which translates into:

$$\Gamma \lesssim \sqrt{|\Delta_1||\Delta_2|}, \quad (4)$$

meaning that the series is always convergent for sufficiently small Γ , provided that Δ_1 and Δ_2 are both finite. This allows us to sum the infinite series and we arrive at $F_{12} = \Gamma[i\omega(\Delta_1 - \Delta_2) + \Delta_2\epsilon_1 + \Delta_1\epsilon_2]/D$, where $D = (\omega^2 + E_1^2)(\omega^2 + E_2^2) - \Gamma^2[2(\epsilon_1\epsilon_2 - \omega^2) - \Delta_2^*\Delta_1 - \Delta_1^*\Delta_2] + \Gamma^4$. The expression for F_{21} is obtained by exchanging the band indices and we can also form the odd and even combinations of F_{12} and F_{21} with respect to the band index:

$$F_{12}^{\text{odd}}(\mathbf{k}, i\omega) = \frac{F_{12} - F_{21}}{2} = i\omega\Gamma(\Delta_1 - \Delta_2)/D \quad (5)$$

$$F_{12}^{\text{even}}(\mathbf{k}, i\omega) = \frac{F_{12} + F_{21}}{2} = \Gamma(\Delta_1\epsilon_{k2} + \Delta_2\epsilon_{k1})/D. \quad (6)$$

The odd-band combination is directly seen to be odd in frequency, whereas the even-band combination has a conventional even-frequency dependence. This is fully consistent with Fermi-Dirac statistics for spin-singlet s -wave superconducting pairing. Furthermore, we see that interband pairing always requires a finite band hybridization and that the odd-interband pairing also requires $\Delta_1 \neq \Delta_2$. Equations (5)-(6) can be Fourier transformed to real space and then evaluated numerically, with the result shown in Fig. 1. By definition, the odd-frequency pairing amplitude must be zero at $\omega = 0$. Close to $\omega = 0$, we find that the leading term in F^{odd} is linear in ω . However, the slope can initially be large and then abruptly change sign to asymptotically go to zero for large ω , resulting in an approximate $1/\omega$ -dependence, which has also been found for some odd-frequency states [53, 54].

By forming an analogue of Eq. (3) for the intraband anomalous Green's function in band 1 we find $F_1 = \{\Delta_1[(i\omega)^2 - E_2^2] - \Gamma^2\Delta_2\}/D$ and the corresponding normal Green's function: $G_1 = \{(i\omega + \epsilon_1)[(i\omega)^2 - E_2^2] - \Gamma^2(i\omega - \epsilon_2)\}/D$. The expressions for F_2 and G_2 are obtained by mutually exchanging band indices. The expressions for the normal Green's functions allow us to compute the DOS using the standard formula:

$$N(E) = -\frac{1}{\pi} \text{Im Tr } G(E + i\delta), \quad \delta \rightarrow 0^+. \quad (7)$$

Here the trace involves a sum over band and spin indices and an integral over k -space. We use similar expressions, but unsummed over the band index, to define the partial DOS N_1 and N_2 .

The total and partial DOS offer a direct connection to experimental measurements on multiband superconductors. In Figs. 2 - 4 we show numerically obtained results for the DOS, explicitly exploring the effect of interband pairing. To most clearly illustrate the effect of interband pairing we use two generic parabolic bands: $\epsilon_j = \hbar^2 k^2/2m_j - \mu_j$, with effective masses $m_1 = 20m_e$,

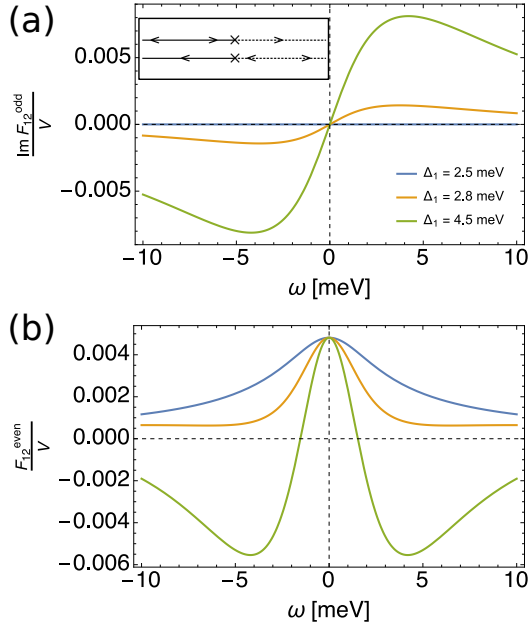


Figure 1: Odd- (a) and even- (b) interband pairing amplitudes in meV per nm³ when $\Delta_2 = 2.5$ meV, $\Delta_1 = 2.5, 2.8, 4.5$ meV (blue, orange, green), and $\Gamma = 3$ meV, with the band structure specified in the main text. Inset: first order hybridization contributions to the interband pairing; $F_1\Gamma G_2$ (top), $-\bar{G}_1\Gamma F_2$ (bottom). Solid (dashed) line represents the propagator in band 1 (2) and \times the hybridization.

$m_2 = 22m_e$ and distances from the bottom of the bands to the Fermi level $\mu_1 = 100$ meV and $\mu_2 = 105$ meV. For this and other band structures we studied, the interband effects are most clearly visible when Γ is comparable to $|\epsilon_1 - \epsilon_2|$ for fixed $k \approx k_F$. The contributions to the DOS are obtained by numerical integration in the range including both Fermi surfaces and we use a smearing parameter $\delta = 0.01$ meV. We have also independently verified the DOS results by exact diagonalization of the Hamiltonian in Eq. (1). In fact, we find a perfect agreement even far beyond the theoretical condition for convergence in Eq. (4).

We here especially showcase that unusual features in the DOS are only seen when the conditions $\Gamma \neq 0$ and $\Delta_1 \neq \Delta_2$ are both satisfied, which are exactly the two key criteria for odd-frequency pairing, see Eq. (5). First, the DOS without any band hybridization, as shown in Fig. 2(a), is just a sum of two BCS spectra with energy gaps $E_{g1} = \Delta_1$ and $E_{g2} = \Delta_2$, respectively, as expected. However, when we turn on hybridization, see Figs. 2(b-d), we see extra, very notable, dips in the DOS located beyond the original gap edges $E_{g1,2}$. These dips, symmetric around zero energy, clearly resemble superconducting gaps with their pronounced BCS-like coherence peaks. However, the DOS in the gap regions are not zero, but instead equal to the partial DOS at these energies. Still, we refer to these features as hybridization-induced gaps.

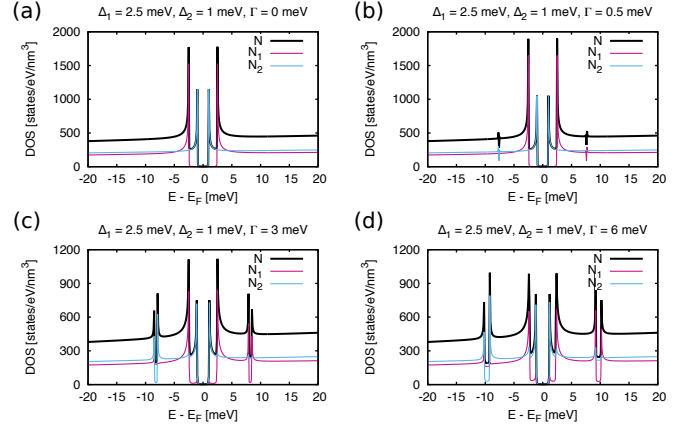


Figure 2: Total (N) and partial densities of states (N_1, N_2) when $\Delta_1 = 2.5$ meV and $\Delta_2 = 1$ meV for different values of $\Gamma = 0, 0.5, 3, 6$ meV (a-d), with the band structure specified in the main text.

The hybridization-induced gaps grow in size and move to higher energies for larger band hybridizations, and we associate these features with interband superconducting pairing. We note that beyond these hybridization-induced gaps, we see no other distinctive features associated with interband pairing. Notably, there are no zero-energy or subgap states, otherwise often associated with odd-frequency pairing [43, 49, 50, 55–58]. Recent works have pointed out that zero-energy states do not always accompany odd-frequency pairing [41, 54, 59, 60], and odd-frequency, odd-interband pairing provides another example when this is not the case.

In Fig. 3 we instead fix $\Gamma = 3$ meV, and $\Delta_2 = 2.5$ meV but vary Δ_1 . Distinct hybridization-induced gaps are present at energies beyond the original gap edges, independent on the relative size of the two original gaps. The only exception is exactly when $\Delta_1 = \Delta_2$, then the hybridization-induced gaps completely disappear, despite the finite band hybridization, see Fig. 3(c). Detuning the value of Δ_1 slightly from that of Δ_2 results in small, but noticeable, dips in the DOS, at the positions where the full gaps develop for increasing differences between Δ_1 and Δ_2 . We thus find that the hybridization-induced gaps are only present in the DOS when both $\Gamma \neq 0$ and $\Delta_1 \neq \Delta_2$. These are exactly the two key criteria for odd-frequency pairing, as seen in Eq. (5). In fact, only the odd-frequency interband pairing disappears at $\Delta_1 = \Delta_2$, the even-frequency part is in general non-zero as soon as $\Gamma \neq 0$. Specifically, the even- and odd-frequency interband pairing amplitudes corresponding to the parameters in Fig. 3(c)-(e) are plotted in Fig. 1. From there it is clear that the even-frequency interband pairing is large and not changing significantly around $\omega = 0$, while the odd-frequency part changes from identically zero in Fig. 3(c) to a notable non-zero derivative at $\omega = 0$ for Figs. 3(d)-(e). We can thus con-

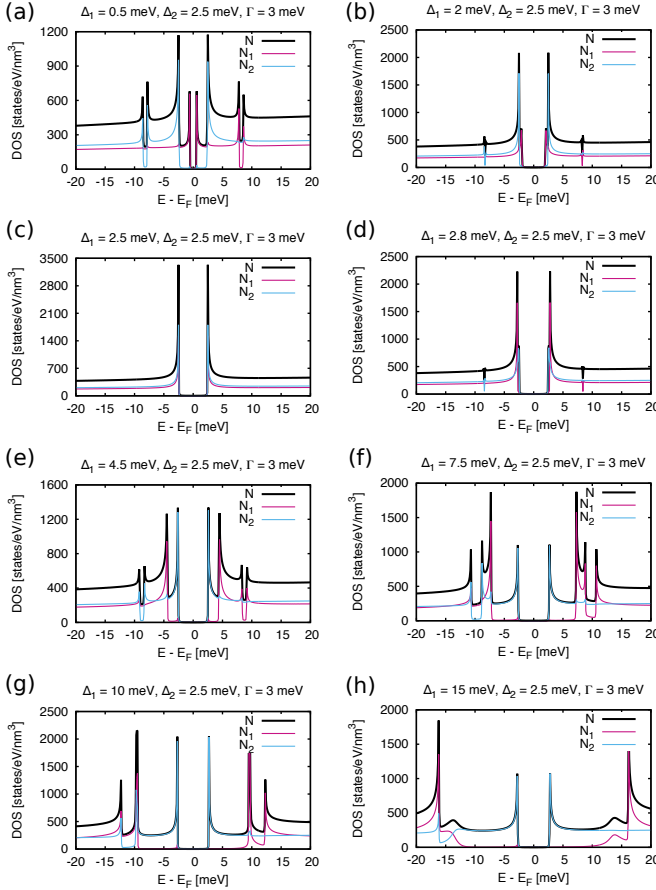


Figure 3: Total (N) and partial densities of states (N_1 , N_2) when $\Delta_2 = 2.5$ meV and $\Gamma = 3$ meV for different values of $\Delta_1 = 0.5, 2, 2.5, 2.8, 4.5, 7.5, 10, 15$ meV (a-h), with the band structure specified in the main text.

clude that odd-frequency interband pairing is necessary for producing the hybridization-induced gaps. Detecting gaps beyond the original two superconducting gaps in multiband superconductors is therefore a clear sign of the presence of odd-frequency pairing. Intriguingly, additional gap features have already been reported in the multiband superconductor $\text{Ba}_8\text{Si}_{46}$ [27].

Finally, we also show that only one band has to be natively superconducting for the hybridization-induced gaps to be present. In Fig. 4 we display how the hybridization-induced gap grows with increasing Γ when $\Delta_2 = 0$. Finite single-particle hybridization Γ results in a proximity-induced gap also in the second band, which is manifested as a gap around zero energy, although always smaller than $E_{g1} = \Delta_1$. For all parameter choices in Fig. 4 the spectrum always has a gap at zero energy, i.e. there are no zero-energy states. This is not clearly seen in Fig. 4(a) due to the finite smearing parameter, but it is clearly visible in exact diagonalization results which do not suffer from the same problem. In addition, a finite Γ results in finite odd-frequency interband pairing, and we consequently also see hybridization-induced

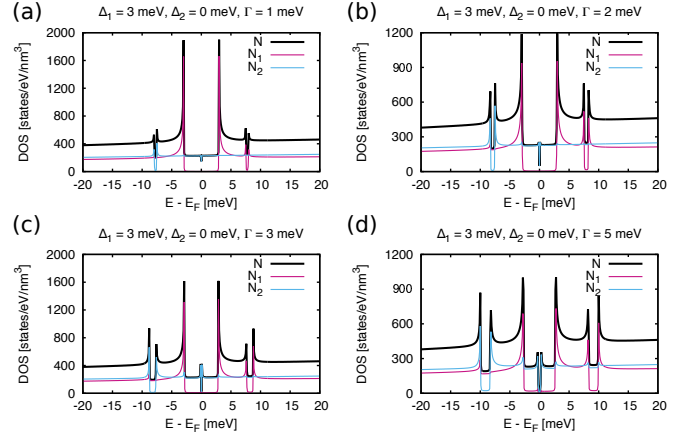


Figure 4: Total (N) and partial densities of states (N_1 , N_2) when $\Delta_1 = 3$ meV and $\Delta_2 = 0$, i.e. only one band with native superconductivity, for different values of $\Gamma = 1, 2, 3, 5$ meV (a-d) with the band structure is specified in the main text.

gaps beyond the Δ_1 gap, which also grow with Γ . In fact, these gaps are much more pronounced than the proximity-induced gap in band 2 at zero energy.

In summary, we have studied the effect of single-quasiparticle hybridization or scattering in a two-band superconductor. By performing perturbation theory to infinite order in the hybridization term, we have obtained the exact, fully frequency dependent, expression for the interband pairing, which can be divided up into odd-frequency odd-interband and even-frequency even-interband pairing. The conditions for finite odd-frequency interband pairing are (a) finite single-quasiparticle hybridization and (b) a non-zero difference between the original superconducting gaps; no applied magnetic field, inhomogeneity, or interface is required. Furthermore, we have shown that the DOS develops non-trivial gaps features with distinct coherence peaks beyond the original gap edges only if the conditions for odd-frequency pairing are satisfied, otherwise the spectrum just a sum of two BCS spectra. Detecting such additional gaps thus provides experimental evidence of odd-frequency pairing in multiband superconductors.

We would like to thank to K. Björnson, D. Kuzmanovski, T. Löthman, and S. Nakosai for valuable discussions. We acknowledge funding from the Wenner-Gren Foundations, the Swedish Research Council (Vetenskapsrådet), the Göran Gustafsson Foundation, and the Swedish Foundation for Strategic Research (SSF) (LK and ABS), and the European Research Council (ERC) DM-321031 (AVB). Work at Los Alamos was supported by the US DOE Basic Sciences E 304 for the National Nuclear Security Administration of the US Department of Energy under Contract No. DE-AC52-06NA25396.

-
- [1] J. Nagamatsu, N. Nakagawa, T. Muranaka, Y. Zenitani, and J. Akimitsu, *Superconductivity at 39 K in magnesium diboride*, Nature **410**, 63 (2001).
- [2] H. J. Choi, D. Roundy, H. Sun, M. L. Cohen, and S. G. Louie, *The origin of the anomalous superconducting properties of MgB₂*, Nature **418**, 758 (2002).
- [3] S. Souma, Y. Machida, T. Sato, T. Takahashi, H. Matsui, S.-C. Wang, H. Ding, A. Kaminski, J. C. Campuzano, S. Sasaki, and K. Kadowaki, *The origin of multiple superconducting gaps in MgB₂*, Nature **423**, 65 (2003).
- [4] Y. Kamihara, T. Watanabe, M. Hirano, and H. Hosono, *Iron-Based Layered Superconductor La[O_{1-x}F_x]FeAs ($x = 0.05 - 0.12$ with $T_c = 26$ K)*, J. Am. Chem. Soc. **130**, 3296 (2008).
- [5] F. Hunte, J. Jaroszynski, A. Gurevich, D. C. Larbalestier, R. Jin, A. S. Sefat, M. A. McGuire, B. C. Sales, D. K. Christen, and D. Mandrus, *Two-band superconductivity in LaFeAsO_{0.89}F_{0.11} at very high magnetic fields*, Nature **453**, 903 (2008).
- [6] G. R. Stewart, *Superconductivity in iron compounds*, Rev. Mod. Phys. **83**, 1589 (2011).
- [7] I. I. Mazin, D. J. Singh, M. D. Johannes, and M. H. Du, *Unconventional Superconductivity with a Sign Reversal in the Order Parameter of LaFeAsO_{1-x}F_x*, Phys. Rev. Lett. **101**, 057003 (2008).
- [8] T. Hanaguri, S. Niitaka, K. Kuroki, and H. Takagi, *Unconventional s-Wave Superconductivity in Fe(Se,Te)*, Science **328**, 474 (2010).
- [9] L. U. L. Shen, N. M. Senozan, and N. E. Phillips, *Evidence for two energy gaps in high-purity superconducting Nb, Ta, and V*, Phys. Rev. Lett. **14**, 1025 (1965).
- [10] E. Boaknin, M. A. Tanatar, J. Paglione, D. Hawthorn, F. Ronning, R. W. Hill, M. Sutherland, L. Taillefer, J. Sonier, S. M. Hayden, and J. W. Brill, *Heat Conduction in the Vortex State of NbSe₂: Evidence for Multiband Superconductivity*, Phys. Rev. Lett. **90**, 117003 (2003).
- [11] G. R. Stewart, *Non-Fermi-liquid behavior of d- and f-electron metals*, Rev. Mod. Phys. **73**, 797 (2001).
- [12] M. Jourdan, A. Zakharov, M. Foerster, and H. Adrian, *Evidence for Multiband Superconductivity in the Heavy Fermion Compound UNi₂Al₃*, Phys. Rev. Lett. **93**, 097001 (2004).
- [13] P. M. C. Rourke, M. A. Tanatar, C. S. Turel, J. Berdeklis, C. Petrovic, and J. Y. T. Wei, *Spectroscopic Evidence for Multiple Order Parameter Components in the Heavy Fermion Superconductor CeCoIn₅*, Phys. Rev. Lett. **94**, 107005 (2005).
- [14] G. Seyfarth, J. P. Brison, M.-A. Méasson, J. Flouquet, K. Izawa, Y. Matsuda, H. Sugawara, and H. Sato, *Multiband Superconductivity in the Heavy Fermion Compound PrOs₄Sb₁₂*, Phys. Rev. Lett. **95**, 107004 (2005).
- [15] R. W. Hill, S. Li, M. B. Maple, and L. Taillefer, *Multiband Order Parameters for the PrOs₄Sb₁₂ and PrRu₄Sb₁₂ Skutterudite Superconductors from Thermal Conductivity Measurements*, Phys. Rev. Lett. **101**, 237005 (2008).
- [16] B. Bergk, V. Petzold, H. Rosner, S.-L. Drechsler, M. Bartkowiak, O. Ignatchik, A. D. Bianchi, I. Sheikin, P. C. Canfield, and J. Wosnitza, *Anisotropic Multiband Many-Body Interactions in LuNi₂B₂C*, Phys. Rev. Lett. **100**, 257004 (2008).
- [17] S. Kuroiwa, Y. Saura, J. Akimitsu, M. Hiraishi, M. Miyazaki, K. H. Satho, S. Takeshita, R. Kadono, *Multigap Superconductivity in Sesquicarbides La₂C₃ and Y₂C₃*, Phys. Rev. Lett. **100**, 097002 (2008).
- [18] A. P. Petrović, R. Lortz, G. Santi, C. Berthod, C. Dubois, M. Decroux, A. Demuer, A. B. Antunes, A. Paré, D. Salloum, P. Gougeon, M. Potel, and Ø. Fischer, *Multiband Superconductivity in the Chevrel Phases SnMo₆S₈ and PbMo₆S₈*, Phys. Rev. Lett. **106**, 017003 (2011).
- [19] S. Deng, L. Viola, and G. Ortiz, *Majorana Modes in Time-Reversal Invariant s-Wave Topological Superconductors*, Phys. Rev. Lett. **108**, 036803 (2012).
- [20] S. Deng, G. Ortiz, and L. Viola, *Multiband s-wave topological superconductors: Role of dimensionality and magnetic field response*, Phys. Rev. B **87**, 205414 (2013).
- [21] H. Suhl, B. T. Matthias, and L. R. Walker, *Bardeen-Cooper-Schrieffer theory of superconductivity in the case of overlapping bands*, Phys. Rev. Lett. **3**, 552 (1959).
- [22] M. E. Zhitomirsky and V.-H. Dao, *Ginzburg-Landau theory of vortices in a multigap superconductor*, Phys. rev. B **69**, 054508 (2004).
- [23] A. Chaves, L. Komendová, M. V. Milošević, J. S. Andrade Jr., G. A. Farias, and F. M. Peeters, *Conditions for nonmonotonic vortex interaction in two-band superconductors*, Phys. Rev. B **83**, 214523 (2011).
- [24] L. Komendová, Y. Chen, A. A. Shanenkov, Milošević, and F. M. Peeters, *Two-band superconductors: Hidden criticality deep in the superconducting state*, Phys. Rev. Lett. **108**, 207002 (2012).
- [25] E. Babaev, J. Carlström, and M. Speight, *Type-1.5 superconducting state from an intrinsic proximity effect in two-band superconductors*, Phys. Rev. Lett. **105**, 067003 (2010).
- [26] J. Carlström, E. Babaev, and M. Speight, *Type-1.5 superconductivity in multiband systems: Effects of interband couplings*, Phys. Rev. B **83**, 174509 (2011).
- [27] Y. Noat, T. Cren, P. Toulemonde, A. San Miguel, F. Debontridder, V. Dubost and D. Roditchev, *Two energy gaps in the tunneling-conductance spectra of the superconducting clathrate Ba₈Si₄₆*, Phys. Rev. B **81**, 104522 (2010).
- [28] Y. Noat, T. Cren, F. Debontridder, D. Roditchev, W. Sacks, P. Toulemonde and A. San Miguel, *Signatures of multigap superconductivity in tunneling spectroscopy*, Phys. Rev. B **82**, 014531 (2010).
- [29] Y. Noat, T. Cren, V. Dubost, S. Lange, F. Debontridder, P. Toulemonde, J. Marcus, A. Sulpice, W. Sacks and D. Roditchev, *Disorder effects in pnictides: a tunneling spectroscopy study*, J. Phys.: Condens. Matter **22**, 465701 (2010).
- [30] H. Schmidt, J. F. Zasadzinski, K. E. Gray, D. G. Hinks, *Break-junction tunneling on MgB₂*, Physica C **385**, 221 (2003).
- [31] D. Mou, R. Jiang, V. Taufour, S. L. Bud'ko, P. C. Canfield, A. Kaminski, *Momentum dependence of the superconducting gap and in-gap states in MgB₂ multi-band superconductor*, arXiv:1504.06347 (2015).
- [32] W. L. McMillan, *Tunneling model of the superconducting proximity effect*, Phys. Rev. **175**, 537 (1968).
- [33] N. Schopohl and K. Scharnberg, *Tunneling density of states for the two-band model of superconductivity*, Solid State Commun. **22**, 371 (1977).
- [34] G. M. Japiassú, M. A. Continentino, and A. Troper, *Mean-field treatment of the hybridization influence on*

- narrow-band superconductivity, Phys. Rev. B **45**, 2986 (1992).
- [35] A. Moreo, M. Daghofer, A. Nicholson, and E. Dagotto, *Interband pairing in multiorbital systems*, Phys. Rev. B **80**, 104507 (2009).
 - [36] V. Cvetkovic and O. Vafeek, *Space group symmetry, spin-orbit coupling, and the low-energy effective Hamiltonian for iron-based superconductors*, Phys. Rev. B **88**, 134510 (2013).
 - [37] T. T. Ong and P. Coleman, *Tetrahedral and Orbital Pairing: A Fully Gapped Scenario for the Iron-Based Superconductors*, Phys. Rev. Lett. **111**, 217003 (2013).
 - [38] A. Hinojosa and A. V. Chubukov, *Gap structure in Fe-based superconductors with accidental nodes: the role of hybridization*, arXiv:1504.02336v1 (2015).
 - [39] W. V. Liu and F. Wilczek, *Interior Gap Superfluidity*, Phys. Rev. Lett. **90**, 047002 (2003).
 - [40] E. Gubankova, W. V. Liu and F. Wilczek, *Breached Pairing Superfluidity: Possible Realization in QCD*, Phys. Rev. Lett. **91**, 032001 (2003).
 - [41] A. M. Black-Schaffer and A. V. Balatsky, *Odd-frequency superconducting pairing in multiband superconductors*, Phys. Rev. B **88**, 104514 (2013).
 - [42] V. L. Berezinskii, *New model of the anisotropic phase of superfluid He^3* , JETP Lett. **20**, 287 (1974) [Zh. Eksp. Teor. Fiz. **20**, 628 (1974)].
 - [43] A. Balatsky and E. Abrahams, *New class of singlet superconductors which break the time reversal and parity*, Phys. Rev. B **45**, 13125(R) (1992).
 - [44] E. Abrahams, A. Balatsky, D. J. Scalapino, and J. R. Schrieffer, *Properties of odd-gap superconductors*, Phys. Rev. B **52**, 1271 (1995).
 - [45] F. S. Bergeret, A. F. Volkov, and K. B. Efetov, *Long-Range Proximity Effects in Superconductor-Ferromagnet Structures*, Phys. Rev. Lett. **86**, 4096 (2001).
 - [46] F. S. Bergeret, A. F. Volkov, and K. B. Efetov, *Odd triplet superconductivity and related phenomena in superconductor-ferromagnet structures*, Rev. Mod. Phys. **77**, 1321 (2005).
 - [47] A. Aperis, P. Maldonado, and P. M. Oppeneer, *Magnetic-Field-Induced Odd-Frequency Superconductivity in MgB_2* , arXiv:1503.05155 (2015).
 - [48] Y. Tanaka and A. A. Golubov, *Theory of the Proximity Effect in Junctions with Unconventional Superconductors*, Phys. Rev. Lett. **98**, 037003 (2007).
 - [49] Y. Tanaka, A. A. Golubov, S. Kashiwaya, and M. Ueda, *Anomalous Josephson effect between even- and odd-frequency superconductors*, Phys. Rev. Lett. **99**, 037005 (2007).
 - [50] Y. Tanaka, Y. Tanuma, and A. A. Golubov, *Odd-frequency pairing in normal-metal/superconductor junctions*, Phys. Rev. B **76**, 054522 (2007).
 - [51] F. Parhizgar and A. M. Black-Schaffer, *Unconventional proximity-induced superconductivity in bilayer systems*, Phys. Rev. B **90**, 184517 (2014).
 - [52] See, e.g., G. D. Mahan, *Many-Particle Physics*, Plenum Publishers, New York (2000).
 - [53] P. Coleman, E. Miranda, and A. Tsvelik, *Possible realization of odd-frequency pairing in heavy fermion compounds*, Phys. Rev. Lett. **70**, 2960 (1993).
 - [54] A. M. Black-Schaffer and A. V. Balatsky, *Odd-frequency superconducting pairing in topological insulators*, Phys. Rev. B **86**, 144506 (2012).
 - [55] T. Yokoyama, Y. Tanaka, and A. A. Golubov, *Manifestation of the odd-frequency spin-triplet pairing state in diffusive ferromagnet/superconductor junctions*, Phys. Rev. B **75**, 134510 (2007).
 - [56] H. P. Dahal, E. Abrahams, D. Mozyrsky, Y. Tanaka, and A. V. Balatsky, *Wave function for odd-frequency superconductors*, New. J. Phys. **1**, 065005 (2009).
 - [57] Y. Asano and Y. Tanaka, *Majorana fermions and odd-frequency Cooper pairs in a normal-metal nanowire proximity-coupled to a topological superconductor*, Phys. Rev. B **87**, 104513 (2013).
 - [58] Y. Tanaka, M. Sato, and N. Nagaosa, *Symmetry and Topology in Superconductors - Odd-Frequency Pairing and Edge States*, J. Phys. Soc. Jpn. **81**, 011013 (2012).
 - [59] A. M. Black-Schaffer and A. V. Balatsky, *Proximity-induced unconventional superconductivity in topological insulators*, Phys. Rev. B **87**, 220506(R) (2013).
 - [60] J. Linder and J. W. A. Robinson, *Anomalous Odd-Frequency Pairing Correlations in Zeeman-split Superconductors*, arXiv:1409.3228 (2014).
 - [61] See Supplementary Material for a derivation.

Band Hybridization Induced Odd-Frequency Pairing in Multiband Superconductors: Supplementary material

In this Supplementary Material we derive in detail the exact result (within perturbation theory) of the interband pairing amplitude in a two-band superconductor with hybridized bands.

The Hamiltonian for a generic multiband superconductor can be written as (same as Eq. (1) in the main text):

$$H = \sum_{k\sigma} \epsilon_{k1} a_{k\sigma}^\dagger a_{k\sigma} + \epsilon_{k2} b_{k\sigma}^\dagger b_{k\sigma} + \sum_{k\sigma} \Gamma(k) a_{k\sigma}^\dagger b_{k\sigma} + \text{H.c.} \\ + \sum_k \Delta_1(k) a_{k\uparrow}^\dagger a_{-k\downarrow}^\dagger + \Delta_2(k) b_{k\uparrow}^\dagger b_{-k\downarrow}^\dagger + \text{H.c.} \quad (\text{S1})$$

It describes two superconducting bands coupled by a hybridization, or scattering, term $\Gamma(k)$, which we treat as a perturbation. We thus start with two copies of the single band superconducting Green's functions (same as Eq. (2) in the main text):

$$\begin{pmatrix} G_j & F_j \\ F_j^\dagger & \bar{G}_j \end{pmatrix} = \frac{1}{(i\omega)^2 - E_j^2} \begin{pmatrix} i\omega + \epsilon_{kj} & \Delta_j \\ \Delta_j^* & i\omega - \epsilon_{kj} \end{pmatrix}, \quad (\text{S2})$$

which we use together with the hybridization term to build up the full Green's functions of the system. Here G is the normal electron propagator, which we schematically denote by \longrightarrow , and \bar{G} is the hole propagator denoted by \longleftarrow . Moreover, F is the anomalous propagator, denoted by \longleftrightarrow , and F^\dagger is its Hermitian conjugate $\longrightarrow\longleftarrow$. We will furthermore use solid lines to denote the propagators in band 1 and dashed lines for band 2. The hybridization term is represented by \times , which always connects two propagators from different bands with the same direction of the arrow (due to momentum conservation).

Now, we want to calculate the interband pairing amplitude F_{12} , which corresponds to the sum of all processes of the type $\longleftarrow\bigcirc\longrightarrow$. The simplest processes, here indicated by the superscript (1), include just one scattering event \times : $F_{12}^{(1)} = \longleftarrow\longrightarrow\longrightarrow\longrightarrow - \longrightarrow\longleftarrow\longrightarrow\longrightarrow = F_1 \Gamma G_2 - \bar{G}_1 \Gamma F_2$. The sign of a particular process is simply given by $(-1)^l$, where l is the number of hole scattering events, i.e. scattering connecting two left-going arrows.

Since F_{12} of any given order has to end with a right-pointing arrow in band two, there are only two possibilities, either it ends with $\times\longrightarrow\longrightarrow$ or with $\times\longleftarrow\longrightarrow$. Similarly, it needs to start with a left-going solid arrow, which also limits the options. By drawing all possible processes and translating them into formulas, we can write:

$$F_{12}^{(n)} = -\bar{G}_1^{(n-1)} \times \longleftarrow\longrightarrow + F_1^{(n-1)} \times \longrightarrow\longrightarrow. \quad (\text{S3})$$

Carrying this procedure one step further, we write $\bar{G}_1^{(n-1)}$ and $F_1^{(n-1)}$ using $F_{12}^{(n-2)}$ and $\bar{G}_{12}^{(n-2)}$:

$$\bar{G}_1^{(n-1)} = F_{12}^{(n-2)} \times \longrightarrow\longrightarrow - \bar{G}_{12}^{(n-2)} \times \longleftarrow\longrightarrow \quad (\text{S4})$$

$$F_1^{(n-1)} = F_{12}^{(n-2)} \times \longrightarrow\longrightarrow - \bar{G}_{12}^{(n-2)} \times \longleftarrow\longrightarrow. \quad (\text{S5})$$

Plugging these into Eq. (S3) we arrive at:

$$F_{12}^{(n)} = \bar{G}_{12}^{(n-2)} [\times\longleftarrow\longrightarrow\longrightarrow\longrightarrow - \times\longrightarrow\longrightarrow\longrightarrow\longrightarrow] + F_{12}^{(n-2)} [\times\longrightarrow\longrightarrow\longrightarrow\longrightarrow - \times\longrightarrow\longrightarrow\longrightarrow\longrightarrow]. \quad (\text{S6})$$

By a similar procedure we get:

$$\bar{G}_{12}^{(n)} = \bar{G}_{12}^{(n-2)} [\times\longleftarrow\longrightarrow\longrightarrow\longrightarrow - \times\longrightarrow\longrightarrow\longrightarrow\longrightarrow] + F_{12}^{(n-2)} [\times\longrightarrow\longrightarrow\longrightarrow\longrightarrow - \times\longrightarrow\longrightarrow\longrightarrow\longrightarrow]. \quad (\text{S7})$$

Thus, we get a closed set of equations if we consider F_{12} and \bar{G}_{12} together, which is easiest done in a matrix formalism. Note that all arrow diagrams can be directly translated to specific formulas using Eq. (2), e.g. $\times\longleftarrow\longrightarrow\longrightarrow\longrightarrow = -\Gamma \bar{G}_1 (-\Gamma) F_2 = (-\Gamma)^2 (i\omega - \epsilon_1) \Delta_2 / \{[(i\omega)^2 - E_1^2][(i\omega)^2 - E_2^2]\}$.

Summarizing, we arrive at the matrix recursion relation in Eq. (3) in the main text:

$$\begin{pmatrix} \bar{G}_{12}^{(n)} \\ F_{12}^{(n)} \end{pmatrix} = g \begin{pmatrix} e & f \\ -f^* & e^* \end{pmatrix} \begin{pmatrix} \bar{G}_{12}^{(n-2)} \\ F_{12}^{(n-2)} \end{pmatrix}, \quad (\text{S8})$$

where $g = \Gamma^2 / [(\omega^2 + E_{k1}^2)(\omega^2 + E_{k2}^2)]$, $e = (i\omega - \epsilon_1)(i\omega - \epsilon_2) - \Delta_1 \Delta_2^*$ and $f = -i\omega(\Delta_1^* - \Delta_2^*) + \Delta_1^* \epsilon_2 + \Delta_2^* \epsilon_1$.

This is a matrix geometric series and is thus easily summed giving:

$$\begin{pmatrix} \bar{G}_{12} \\ F_{12} \end{pmatrix} = q \begin{pmatrix} 1 - ge^* & gf \\ -gf^* & 1 - ge \end{pmatrix} \begin{pmatrix} \bar{G}_{12}^{(1)} \\ F_{12}^{(1)} \end{pmatrix}, \quad (\text{S9})$$

where $q = [(1 - ge)(1 - ge^*) + g^2 |f|^2]^{-1}$, $\bar{G}_{12}^{(1)} = \longleftarrow\longrightarrow\longrightarrow\longrightarrow - \longrightarrow\longleftarrow\longrightarrow\longrightarrow = \Gamma[\Delta_1 \Delta_2^* - (i\omega - \epsilon_1)(i\omega - \epsilon_2)] / [(\omega^2 + E_1^2)(\omega^2 + E_2^2)]$. Some terms cancel and we get $F_{12} = q F_{12}^{(1)}$. Finally $F_{12} = \Gamma[i\omega(\Delta_1 - \Delta_2) + \Delta_2 \epsilon_1 + \Delta_1 \epsilon_2] / D$, where $D = (\omega^2 + E_1^2)(\omega^2 + E_2^2) - \Gamma^2[2(\epsilon_1 \epsilon_2 - \omega^2) - \Delta_2^* \Delta_1 - \Delta_1^* \Delta_2] + \Gamma^4$.

For the normal propagator G_1 , needed for calculating the DOS, we create a matrix equation together with F_1^\dagger , otherwise the procedure proceeds in the same manner as above.